T.2: Development of an infra-red free electron laser (IR-FEL) and its user facility at RRCAT

Bhaskar Biswas, Arvind Kumar, M. K. Chattopadhyay and K. K. Pant*
Free Electron Laser and Utilization Section
**Email: kkpant@rrcat.gov.in*

Abstract
The infra-red free electron laser (IR-FEL) at Raja Ramanna Centre for Advanced Technology (RRCAT) has been designed to deliver 30 mW of continuous wave (CW) average infra-red (IR) power output in the wavelength range of 12.5-50 µm, with a peak power > 2.5 MW in 10 ps pulses. Since the first reported measurement of build-up of coherence in the IR-FEL setup in 2016, the injector system of the IR-FEL has been upgraded and saturation of lasing has been achieved with ~ 30 mW of CW average output power at a duty cycle of operation five times lower than the design value. This article presents the status of development of the IR-FEL facility, and discusses results obtained in the different stages of commissioning of the machine. The tunability of the IR-FEL and its pulse structure makes it a unique tool for research particularly in areas that require precise tuning of photon energy to either excite or probe some phenomena, and also for time dependent measurements. Salient features of a user facility that has been built for materials research in low temperature and high magnetic field environment have also been presented in this article.

1. Introduction

A free electron laser (FEL) is a source of tunable coherent electromagnetic radiation, which is generated by the propagation of a relativistic electron beam through a spatially periodic arrangement of magnets called an undulator. Conventionally, FELs are operated either in an oscillator configuration by employing an optical cavity, or in an amplifier configuration to amplify a seed radiation. Since the first successful operation of a FEL by Madey in 1976, many FELs have been built worldwide at wavelengths covering a large portion of the electromagnetic spectrum from millimeter to ultraviolet wavelengths. In the last couple of decades, there has been exceptional progress in the operation of FELs at hard x-ray wavelengths too in the self-amplified spontaneous emission (SASE) configuration. Starting from shot noise, lasing is achieved in this configuration through the interaction of an intense ultra-short electron bunch with the spontaneous radiation emitted by it, as they co-propagate through a long undulator. However, from the cost-to-benefit considerations, FELs are currently being designed and developed worldwide primarily in two wavelength regimes where other sources of intense, coherent radiation are either not present, or are not very efficient. These regions are: (1) IR/THz region and (2) X-ray region. Several FELs operating in both these wavelength regions have been setup worldwide as user facilities. While IR/THz FELs require modest facilities with electron beam energies of ~5-15 MeV and undulator lengths of 1.5-3.0 m, X-ray FELs require large facilities with multi-GeV electron beam energies and undulator length of ~100-200 m. To reduce the cost, some modern X-ray FELs have also been built by employing modest electron beam energy of ~400-800 MeV and relatively short undulator lengths by employing novel schemes like seeding and harmonic generation.

The FEL program at RRCAT began with the development of a compact ultrafast terahertz-FEL (CUTE-FEL), where the first signature of build-up of coherence was observed in 2012 [1]. This was a technology demonstrator machine where all the subsystems like the injector linac components, undulator, optical cavity, etc. were developed fully in-house. Learning from this experience, design and development activity began for the IR-FEL, with an aim to build the FEL and a commensurate user facility for IR-THz spectroscopy of materials using the FEL radiation. This machine was commissioned in 2016 and first signature of build-up of coherence was observed in November 2016 [2]. The injector linac system was subsequently upgraded and saturation of lasing of the IR-FEL at 28 µm wavelength was achieved in 2020 with a measured CW out-coupled power of 7.3 mW. With further optimization of the injector, transport line magnets and optical cavity parameters, a CW average power up to 30 mW has been achieved, which is around 5 times higher than the design power output for the full duty cycle of operation of the machine. Characterization of the electron and optical beam parameters of the IR-FEL has been done, achieving good agreement of the measured laser parameters with those predicted by the FEL simulations. The FEL radiation has been transported to the user station through a 50 m long optical beam transport line, and first user experiments have been done using the FEL light.

A summary of the FEL design parameters and the results obtained in the first lasing experiments is given in the next Section. Section 3 discusses the upgrade of the IR-FEL injector system and the low energy electron beam transport system, which led to the saturation of lasing of the IR-FEL. Section 4 discusses results from experiments performed after optimization of the operation parameters, and results from the characterization of the electron and FEL optical beam. Salient features of the user facility developed to use the IR radiation from the FEL, and results from first experiment on characterization of the FEL radiation using a standard substrate sample, are presented in Section 5. The article concludes with a discussion of the plans for the future in Section 6, and a summary of results obtained in Section 7.

2. IR-FEL design parameters and first lasing

The IR-FEL at RRCAT is designed to operate in an oscillator configuration to generate radiation in the 12.5-50.0 µm wavelength range by employing an electron beam of 15-25 MeV energy and a 2.5 m long, 50 period pure permanent magnet (PPM) planar undulator with undulator parameter lying in the range 0.54-1.26. The pulse structure of the output radiation from an FEL mimics the electron beam pulse structure. Figure T.2.1 shows the pulse structure of the IR-FEL radiation, which has bursts of 10 ps full width at half maximum (FWHM) micro-pulses repeating at 29.75 MHz or 59.5 MHz (user-settable) for a macro-pulse duration adjustable from 4-10 µs. The pulse repetition rate (PRR) is adjustable from 1-10 Hz.

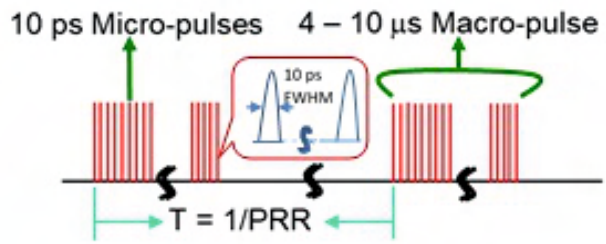

Fig. T.2.1: Pulse structure of IR-FEL radiation.

The goal for the first phase of commissioning of the IR-FEL was to achieve a CW average power of 30 mW at ~25 µm wavelength using electron beam micro-pulses at 29.75 MHz for a macro-pulse duration of 9 µs with a PRR of 2 Hz. The target for the ongoing second phase is to increase the CW power output to more than 100 mW, which will be achieved by a combination of increasing the electron bunch burst frequency from 29.75 MHz to 59.5 MHz and the PRR from 2 to 4 Hz.

Installation of the IR-FEL sub-systems inside a 60 m long radiation shielded area was done in 2015, and commissioning experiments began in 2016 leading to the first observation of build-up of coherence in the setup in November 2016 at a wavelength of 36 µm. A typical growth curve of intra-cavity power in an oscillator FEL, which is the increase in power with the number of round-trips made by the optical pulse in the cavity, also called as the pass number, is shown in Figure T.2.2. The initial portion of the growth curve shows a slow growth of FEL power due to spontaneous radiation. After a few round-trips, the electrons in each micro-pulse start getting re-distributed through their interaction with the undulator magnetic field and the electromagnetic field of the amplified spontaneous radiation, and micro-bunching takes place at the wavelength of the electromagnetic radiation. Power output in this region shows a steep growth with pass number due to the coherent addition of power from the micro-bunches in a micro-pulse. This results in several orders of magnitude higher power than the spontaneous emission from the electrons in the micro-pulse. Typically, saturation of the FEL power growth occurs before perfect micro-bunching is achieved. The measured out-coupled IR power in the first commissioning experiments on the IR-FEL setup was estimated to be 10^5 times higher than the spontaneous emission power expected for the electron beam used in these experiments, which was the first signature of lasing in the setup [2]. This power gain was obtained by the optimization of the optical cavity length for detuning in very small steps of a few mm, and the large power gain was lost as expected with a detuning of the cavity length by ~ 20 µm.

The injector system used in the experiments employed a re-furbished thermionic electron gun from the CUTE-FEL setup, a 476 MHz sub harmonic pre-buncher cavity and two cascaded 12-cell plane wave transformer linac structures [3], all developed in-house. This injector system delivered an electron beam of 18.4 MeV energy, 0.26 nC charge per micro-pulse with ~50 mm.mrad normalized root mean square (RMS) emittance [4]. FEL simulations considering the electron beam parameters achieved in these experiments showed a reasonably good agreement with the measured IR radiation

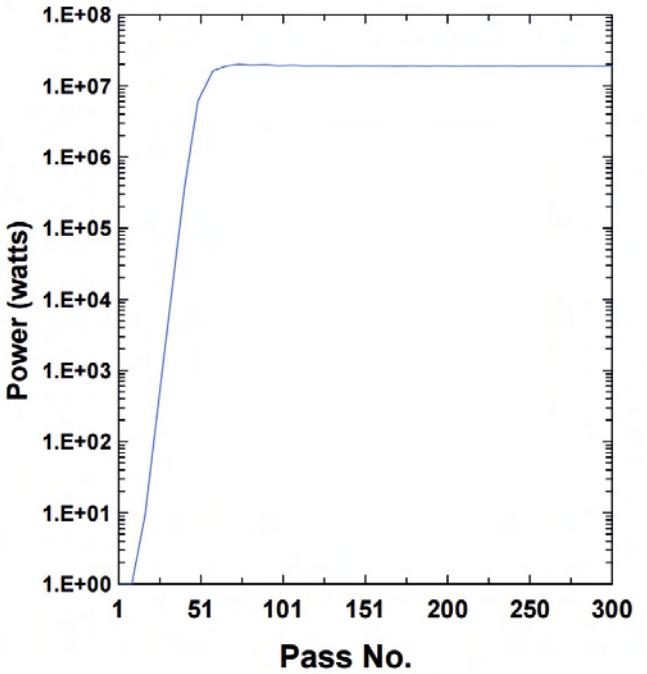

Fig. T.2.2: Growth of FEL power with pass number.

output from the FEL, and also indicated that further enhancement of power output from the FEL leading to saturation of lasing could not be achieved with this injector system.

Lasing over the design wavelength range of 12.5-50 µm requires an electron beam of energy variable from 15-25 MeV, with a peak micro-pulse charge >0.3 nC/micro-pulse, normalized emittance <50 mm.mrad and a relative energy spread of <0.5%. Further, since the IR-FEL operates in an oscillator configuration with around 50-80 round-trips required to achieve saturation, the stability of the microwave power fed to the accelerating structures is very important since instabilities can cause a jitter in the mean energy of the accelerated electron bunches as well as in the arrival time of the micro-bunches at the undulator entry, thereby adversely affecting the process of lasing. This required an upgrade of the injector system of the IR-FEL to deliver the design electron beam essential to achieve saturation.

3. Upgrade of the IR-FEL injector system: design and commissioning

In order to ensure achievement of the desired electron beam parameters for the IR-FEL, the injector system upgrade was designed through simulations to deliver ~0.75 nC charge per micro-pulse with the desired electron beam energy and relative energy spread. The design simulations considered an electron gun capable of delivering up to 1.5 nC charge in 1 ns FWHM pulses at 90 keV, with a normalized RMS emittance smaller than 20 mm.mrad.

For efficient charge transmission through the injector linac system, each 1 ns FWHM, 90 keV electron bunch from the gun is bunched to ~20 ps by employing a combination of a sub-harmonic pre-buncher (SHPB) cavity at 476 MHz and a

fundamental frequency pre-buncher (FFPB) cavity at 2856 MHz, before injection into an accelerating buncher (AB) at 2856 MHz to further bunch the electron bunches to ~10 ps while simultaneously accelerating them to ~4 MeV energy. A 3 m long, travelling wave (TW) main linac (ML) structure accelerates these bunches to the desired energy of 15-25 MeV when powered at appropriate level through the high power microwave system. A new low energy beam transport (LEBT) line was designed with 19 pancake coils for the transverse confinement of the charge during the bunching and acceleration [5].

3.1 Thermionic electron gun with variable burst frequency: design parameters & qualification

A new triode type thermionic electron gun with a gridded dispenser cathode (Thales, France) was installed in the upgraded IR-FEL injector system. Considering that the optical cavity of the IR-FEL is designed to be 5.04 m long with a round-trip time of 33.613 ns for optical pulses in the cavity, the electron gun was designed to have a burst frequency of 29.75 MHz (1/33.613 ns) so that the spacing between micro-pulses exactly matches the round trip time of optical pulses in the cavity. The chosen frequency is also an exact sub-multiple of the two frequencies employed in the injector linac system – 476 MHz for the SHPB and 2856 MHz for the other three cavities. The burst width is user settable from 1-10 μs with a PRR variable from 1-25 Hz.

As an option aimed at attaining higher CW average power output from the FEL, the electron gun has provision for operation at two times and four times the fundamental burst frequency, i.e., at 59.5 MHz and 119 MHz, both of which are also exact sub-harmonics of 476 MHz as well as of 2856 MHz. This is essential to maintain a precise phase relationship between the all electron micro-bunches in each macro-pulse with the RF and microwave power in the four different cavities employed in the injector linac system.

The electron gun was qualified by measuring the charge per pulse, pulse width, and beam emittance. The charge per pulse was measured with an integrating current transformer (ICT) from M/s Bergoz Instrumentation, France and the bunch length of 1 ns FWHM was measured using an indigenous wall current monitor (WCM). For a pulse width setting of 0.995 ns on the grid-pulser of the gun, the measured pulse width was ~0.89 ns with a charge/pulse of ~1.5 nC. Emittance of the 90 keV beam was measured by employing a solenoid scan method, which involves the comparison of the measured variation of the beam envelope for different solenoid settings with the theoretical variation of the beam envelope for the same solenoid settings, but considering different initial emittances for the electron beam. The actual emittance is the value where the best agreement is observed between the measured and theoretical plots. For 1.5 nC per bunch, the RMS normalized emittance was measured to be between 15-20 mm.mrad [6,7]. Figure T.2.3 shows the acquired electron bunch image in the two orthogonal planes, and Figure T.2.4 shows the measured and fitted variation of beam envelopes for the electron beam during the solenoid scan for emittance measurement.

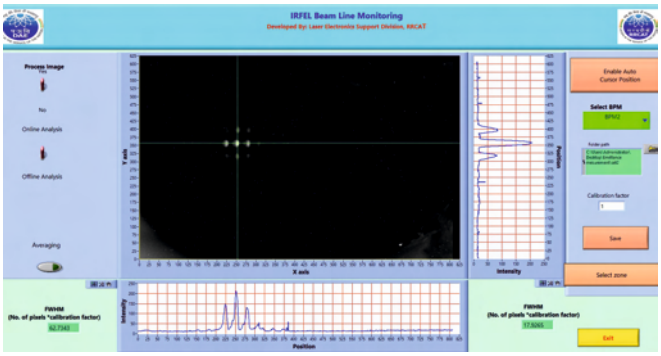

Fig. T.2.3: Transverse profile of the 90 keV beam, and Gaussian fit on horizontal and vertical planes.

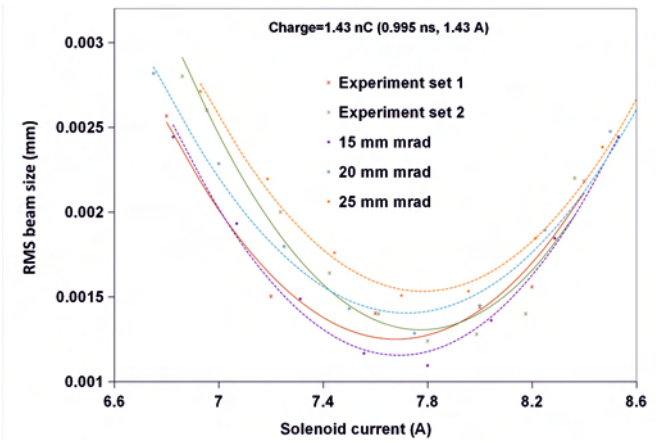

Fig. T.2.4: Variation of 90 keV beam size with solenoid current during emittance measurement.

3.2 Injector linac system upgrade

Upgrade of the injector linac system envisaged the use of the 476 MHz SHPB cavity deployed earlier with three new cavities – FFPB, AB and ML (RadiaBeam Technologies, USA). Considering that a higher charge per pulse from the electron gun was to be transported through this system, a new LEBT was designed and implemented along with the injector system upgrade. Figure T.2.5 shows a schematic of the designed upgrade for the injector system and the new LEBT, and Figure T.2.6 shows a view of the upgraded injector linac system with the LEBT.

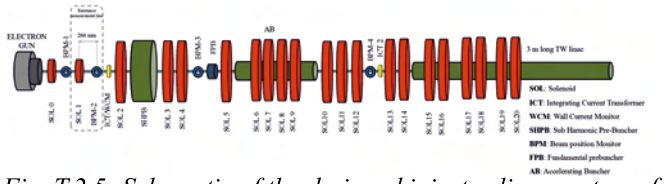

Fig. T.2.5: Schematic of the designed injector linac system of the IR-FEL after the upgrade.

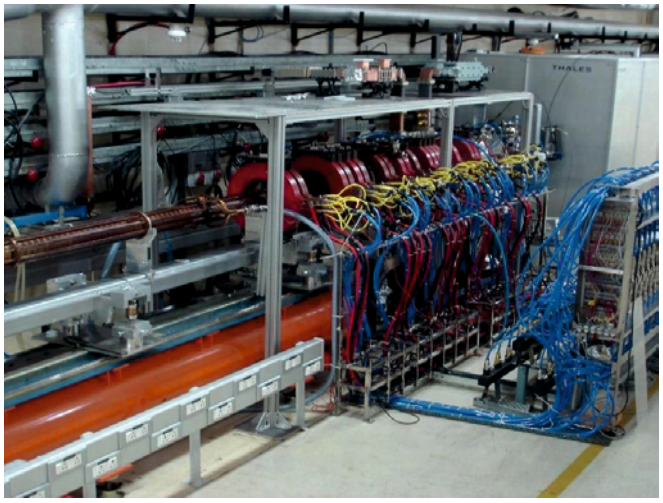

Fig. T.2.6: A view of the upgraded IR-FEL injector linac system.

The radio frequency and microwave power systems of the IR-FEL injector employs a common low level radio frequency (LLRF) system to generate phase-locked seed signals at 476 MHz and 2856 MHz, which are subsequently amplified to appropriate levels by dedicated amplifier systems for the different cavities employed in the IR-FEL injector linac. The LLRF system also generates a clock signal at 476 MHz for the thermionic electron gun, and a 10 MHz reference signal for the trigger and timing generator employed in the IR-FEL setup.

The SHPB is powered by a 3 kW, 50 μs pulsed RF system, the FFPB is powered by a 2 kW, 30 μs pulsed microwave system and the AB and ML are powered by a single klystron based system delivering ~10 MW peak power in 10 μs pulses to the AB. Power from the output port of the travelling wave AB is transported to the ML through a high power microwave line, with provision for varying the power and phase of the microwaves delivered at the ML input port.The design of the LEBT evolved from the beam dynamics simulations for the upgraded injector system with high charge per pulse from the electron gun. The electron bunches have an energy of 90 keV up to the AB entry, while the SHPB and FFPB structures together compress the 1 ns bunch from the electron gun to ~20 ps at the AB entry, causing very significant build-up of space charge forces. The magnetic field profile in the LEBT was tailored to provide transverse confinement to this non-relativistic electron beam in the low energy region, and also in the AB and initial portion of the ML region, where each bunch is further bunched and accelerated.

The IR-FEL optical cavity is 5.04 m long, which translates to a round trip distance of 10.2 m and a round-trip time of 33.613 ns for the optical pulse in the optical cavity. Since lasing action in a FEL is through repeated interactions of this optical pulse with a train of electron bunches, the spacing of the micro-bunches from the electron gun is exactly equal to this round-trip time of optical pulses, which corresponds to a burst frequency of 29.75 MHz. The first stage of commissioning of the upgraded injector linac system for the IR-FEL has been done with a burst frequency of 29.75 MHz and at a PRR of 2 Hz.

The duty-cycle of the IR-FEL setup can be increased either by increasing the PRR of operation, or by increasing the burst frequency from the electron gun. Increasing the PRR of operation has no implications on the optimization of the settings of the injector linac system or the LEBT, and only requires the RF and microwave systems to be able to support operation up to 10 Hz in the first phase and up to 25 Hz in the second phase of commissioning. However, operation of the electron gun with a higher burst frequency has a serious implication on the beam-loading in the injector linac system. Beam dynamics simulations have been performed and schemes have been evolved to compensate the effects of beam loading in the accelerating structures with a burst frequency of 59.75 MHz (2×29.75 MHz) and 119 MHz (4×29.75 MHz). These will be employed in the future in experiments to increase the CW average power output from the FEL.

After a period of RF conditioning of the upgraded injector linac system, beam experiments performed in 2019 resulted in the successful acceleration of 0.69 nC charge/pulse to an energy of ~24 MeV with a RMS relative energy spread, $\Delta E/E \leq 1.5\%$. More details about the upgraded system are given in Ref. [8].

3.3 Saturation of lasing of the IR-FEL

The first observation of build-up of coherence in the IR-FEL setup in 2016 was made with an electron beam of 18.4 MeV energy, 0.26 nC charge per micro-pulse with ~50 mm.mrad normalized RMS emittance and 0.75% relative energy spread. As discussed earlier in Section 2, the time evolution of FEL power for an oscillator FEL shows an initial period of very slow growth followed by a period where the build-up of coherence, or lasing, results in a steep rise in the power by several orders of magnitude. The process of lasing of the FEL subsequently saturates due to the effects of slippage and high energy spread induced in the electron bunches due to the FEL interaction. The electron beam parameters in the first lasing experiments were not optimum to take the lasing process up to saturation, and the out-coupled power achieved then corresponded to a power gain of ~10^5 times as compared to the expected spontaneous radiation power. This was around three orders of magnitude lower than the power expected at saturation of lasing, primarily on account of low charge per micro-pulse, or peak current, with the desired electron beam quality.

The first lasing experiments after commissioning of the upgraded injector linac system were performed with a 5 μs long electron macro-pulse at 24 MeV with ~0.69 nC charge/micro-pulse at a PRR of 2 Hz to achieve a CW average out-coupled power of ~7 mW [6]. This translates to a peak out-coupled power of >4 MW in 10 ps long pulses.

A view of the FEL power output measured using a laser power meter (Make: Ophir, Model: 3A-P-THz) is shown in Figure T.2.7, which also shows the 3D transverse optical mode profile measured using a Pyrocam (Make: Ophir Spiricon, Model: Pyrocam IV) IR camera. A Gaussian-like profile is obtained in both transverse directions, with a distortion due to the out-coupling of FEL power through a hole in the downstream mirror.

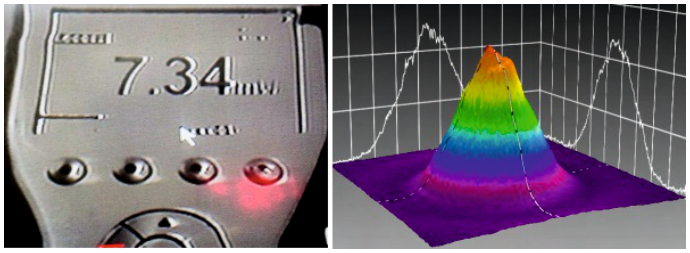

Fig. T.2.7: The measured CW average FEL power by the power meter (left) and the 3D transverse profile of the out-coupled FEL pulse (right).

Lasing of an FEL critically depends upon the peak current, the relative energy spread and jitter in mean energy of the micro-pulses. For an oscillator FEL, the arrival time of micro-pulses at the undulator is also a critical parameter. Though emittance is also important, lasing of the FEL is relatively more tolerant to poor emittance as compared to poor energy spread or mean energy jitter. FEL simulations were performed using the code GINGER [9] to compare the experimental results with predictions from simulations considering the measured values of energy of the electron beam, undulator parameter and charge/micro-pulse with 1.5% relative energy spread, as per the opening width of the energy selecting slit incorporated in the transport line. These simulations do not consider the effect of jitter in mean energy or arrival time of the micro-pulses at the undulator. In the measured charge that is transported up to the undulator, the fraction that falls within 0.5% relative energy spread in 10 ps contributes most effectively to lasing. With a lower peak current or a higher relative energy spread, gain per pass is lower leading to a longer start-up time of the FEL. A reasonably good agreement was obtained between the experimental results and FEL simulations considering experimental parameters.

The synchronism between the successive electron micro-pulses and the optical pulse as they co-propagate through the undulator and exchange energy is another important parameter for lasing of an FEL. This is optimized experimentally by varying the optical cavity length in very small steps of the order of 1 mm. The variation of the FEL power with the detuning of the optical cavity from the ideal length gives the detuning curve of the FEL, and the width of the detuning curve tells us about the process of lasing. A wider detuning curve indicates better electron beam quality resulting in higher output power from the FEL. Typical detuning curves obtained during initial commissioning of the upgraded injector system, and after its optimization, are shown in Figure T.2.8.

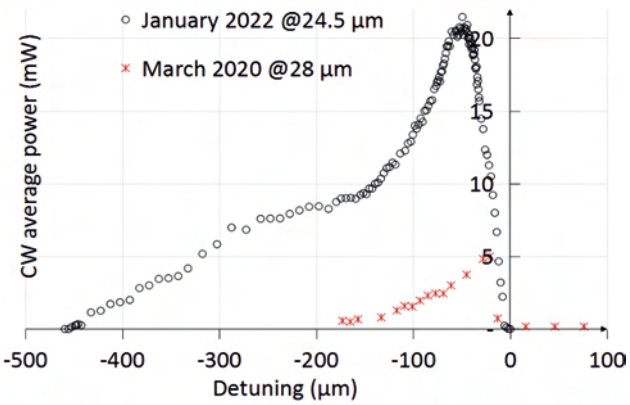

Fig. T.2.8: IR-FEL detuning curve before and after the optimization of injector system and transport line parameters.

In the absence of diagnostics to directly measure the micro-pulse width of the electron bunches and the relative energy spread therein, a parametric study was performed through FEL simulations considering experimental parameters for the beam energy and undulator parameter, but with different values of peak current and relative energy spread, to arrive at estimated values of peak current and relative energy spread in the micro-pulses for which simulations give values of CW average out-coupled power and the detuning curve similar to the experimentally measured values. Based on this, it is estimated that lasing of the IR-FEL was achieved with a peak charge/micro-pulse of ~0.5 nC with an energy spread of ≤0.65%.

4. Optimization of the IR-FEL operating parameters for enhanced lasing

After experiments for the optimization of the injector system, the LEBT, the high energy beam transport (HEBT) line, the injection of the electron beam into the optical cavity and the optical cavity parameters, the electron beam macro-pulse width was increased from 4 µs to 8.5 µs, with a measured charge/micro-pulse exceeding 0.88 nC within a relative energy spread window of <0.75%, as per the opening width of the energy selecting slit. This resulted in lasing of the IR-FEL with a CW average out-coupled power of ~30 mW at a PRR of 2 Hz. It may be noted here that the IR-FEL was designed for a CW average out-coupled power of 30 mW at 10 Hz and 10 µs macro-pulse width, which has been successfully achieved with a five times lower duty cycle.

Detailed calibration of the electron beam and the FEL radiation was performed, and lasing of the FEL was characterized through a measurement of the detuning curve as well as the start-up time using a fast Mercury Cadmium Telluride (MCT) detector (Make: InfraRed Associates Inc., USA, Model: FTIR-24-0.25). The higher peak current achieved in the experiments resulted in a larger width of the detuning curve, as predicted by simulations. The measured start-up time of 2.1 µs is also in a reasonably good agreement with the predicted value of 1.8 µs from FEL simulations, considering 0.65 nC charge per micro-pulse with ~0.5% relative energy spread, which is a significant

improvement in electron beam quality over the values achieved in 2020 after commissioning of the upgraded injector system. The measured width of the detuning curve achieved in 2022 is also in good agreement with the predictions from simulations considering the electron beam parameters discussed above. The green trace in Figure T.2.9 shows the FEL macro-pulse measured using a MCT detector, with the falling edge indicating startup time, the flat-top region indicating the saturated power output, and the rising edge after the pulse indicating cavity quality.

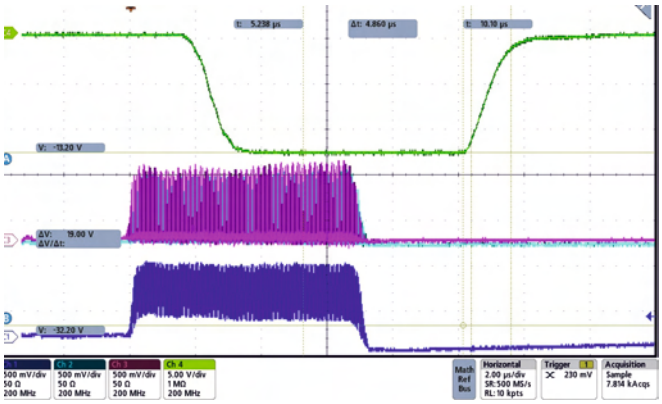

Fig. T.2.9: The FEL radiation macro-pulse (green) and the electron beam pulses (magenta and blue) at the exit of linac and after first bend, respectively.

An important property of an FEL is the tuning of its operating wavelength by varying the electron beam energy as well as the undulator parameter. The wavelength of the IR-FEL has been successfully tuned from 12.5-40.0 μm by a combination of the above two tuning parameters, as shown in Figure T.2.10.

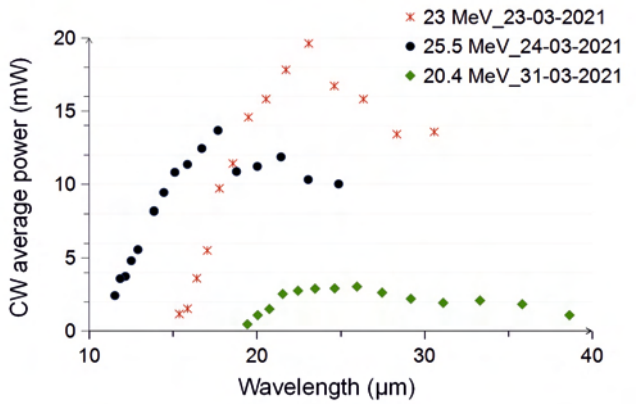

Fig. T.2.10: Tunability of laser wavelength via continuous variation of undulator gap at different electron beam energies.

The wavelength of the out-coupled FEL radiation λ_R is conventionally determined by using the experimental parameters for the electron beam energy (in terms of the relativistic gamma factor γ), the undulator period λ_u and the RMS value of the undulator parameter K_u in the FEL equation:

$$\lambda_R=\lambda_u(1+K_u^2)/2\gamma^2 \quad (1)$$

Here, the energy of the electrons is determined from the setting of the bending magnet for the fixed bending radius in the FEL transport line.

A calibration of the wavelength of FEL radiation determined by the above method has been done by measuring the transmission spectra of a Polymethylpentene window (Trade name TPX of Tydex Optics, Russia) with the FEL radiation over a wavelength range of 15-32 μm, and comparing it with the transmission spectra obtained using a Fourier Transform Infra-Red (FTIR) spectrometer (Bluesky Spectroscopy, Canada). A good agreement was obtained after a small correction in the beam energy used in the FEL equation. Figure T.2.11 shows the two transmission spectra for the same window after the energy correction.

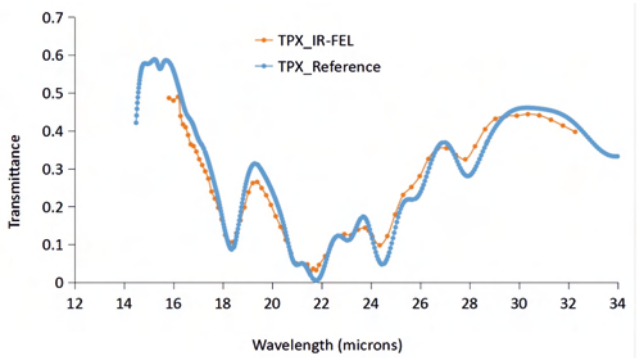

Fig. T.2.11: Transmission spectra of a TPX window using the FEL radiation and an FTIR spectrometer.

Emittance of the accelerated electron beam has been measured to be 67 mm.mrad and 80 mm.mrad in the horizontal and vertical planes, respectively for the electron beam that led to lasing of the IR-FEL with ~0.9 nC charge per micro-pulse [10] before energy analysis. Table T.2.1 summarizes the design and achieved values for different IR-FEL parameters from the two commissioning stages following the injector system upgrade.

Table T.2.1: A summary of the design and achieved parameters for the IR-FEL setup.

Parameter	Design Values	Achieved Values	
		2020	2022
Energy (MeV)	15-25	18-25	18-25
Wavelength (μm)	12.5-50.0	28	12.5-40.0
CW Laser power (mW @ 2 Hz)	6	~ 6	30
Charge (nC in dE/E 0.5%)	0.86	~ 0.50 Estimated	~ 0.65 Estimated
Emittance H/V (mm.mrad)	30/30	110/168	67/80
Cavity detuning length (μm)	31	37	130
Electron beam macro-pulse (μs)	10	5	8.5

5. Experiments at the user station using the first FEL light

The IR radiation from the FEL is transported over a distance of 50 m to the user area through an optical beam transport line flushed with dry nitrogen. Before transport, the M^2 parameter of the out-coupled FEL radiation has been measured inside the radiation shielded area to be <1.1.

The IR-FEL user facility has provision to perform IR/THz spectroscopy of materials in low temperature (down to 3 K) and high magnetic field (up to 7 T) environment. This facility has in-built laboratory sources capable of generating IR/THz radiation from 5-3000 μm wavelength, and a Fourier transform spectrometer (FTS). The first experiments using FEL light were aimed at studying the transmission of the IR radiation through materials under study in a low temperature and high magnetic field sample environment. The experimental layout is shown in Figure T.2.12. For these experiments, the FEL beam was split using a Si beam-splitter and one part of the beam was aligned into a Deuterated *l*-alanine doped Triglycine Sulfate (DTGS) detector. The detector was installed on a Low Density Poly Ethylene (LDPE) chamber (as shown in Figure T.2.13) pressurized using dry-nitrogen gas. The DTGS detector measures the intensity of the direct FEL beam before entering the user station. The remaining part of the beam was bent using gold coated copper mirrors installed inside the same LDPE chamber and routed into the magneto-optical cryostat.

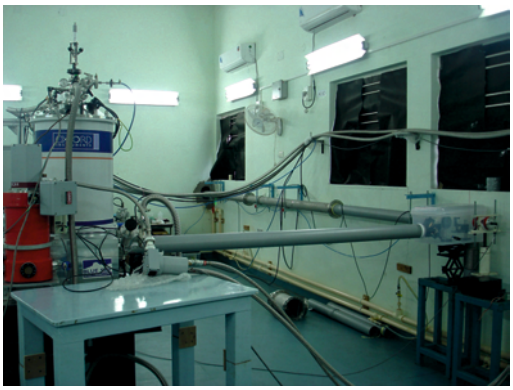

Fig. T.2.12: Beamline coupling of the FEL light to the magneto-optical cryostat based user station.

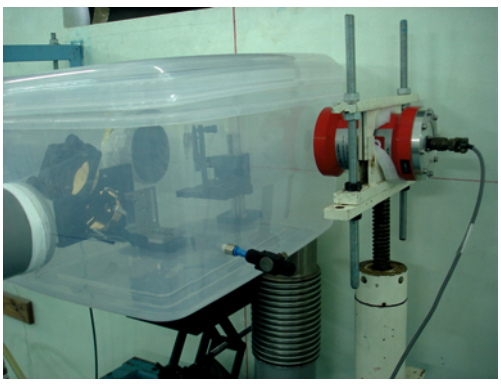

Fig. T.2.13: Nitrogen purged LDPE box housing the DTGS detector beam-splitter and gold mirrors for splitting and coupling the FEL light to the magneto-optical cryostat.

The FEL beam was aligned for transmission across a Si standard sample placed inside the cryostat, and the transmitted signal was measured using a liquid nitrogen cooled MCT detector as shown in Figure T.2.14. Simultaneous data acquisition from the DTGS and MCT detectors was done using a software developed in-house. The frequency of the FEL beam was varied by changing the undulator gap, and the frequency dependence of transmissivity of the sample was measured using the FEL light. These results were compared with the frequency dependence of transmission obtained using the laboratory based FTS set-up. The two results exhibit reasonable agreement, as shown in Figure T.2.15.

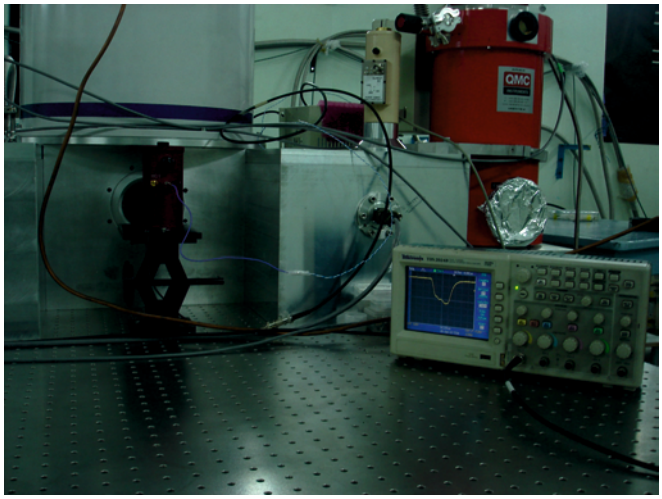

Fig. T.2.14: Measurement (using MCT detector) of FEL light transmission through Si sample placed inside a magneto-optical cryostat system.

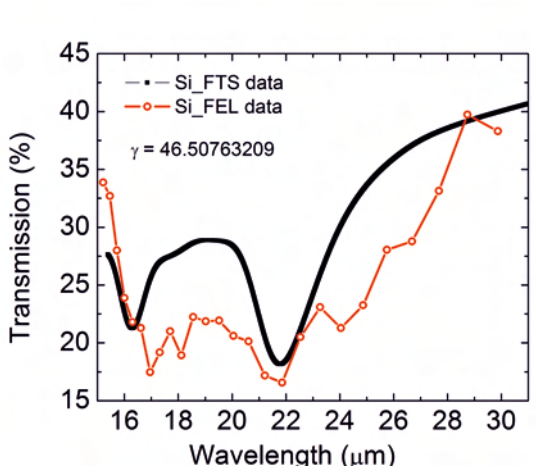

Fig. T.2.15: Wavelength dependent transmission of FEL light through Si standard sample and comparison with FTS results.

6. Future plans

Presently, efforts are underway to reduce losses in the FEL beam transmission from the radiation shielded area to the user area. An adaptive section is proposed to be added inside the

radiation shielded area, as well as in the laser diagnostic room before the user lab, to reduce the beam size. The existing 75 mm diameter mirrors at locations of 45° or greater angle of incidence on the optical elements are proposed to be replaced with larger mirrors of 90 mm × 130 mm size. Another beam reducer is proposed to be setup at the user room to focus the beam to under 10 mm at the user table for experiments. This modification has been designed using the code FINESSE [11].

An upgrade of the optical cavity is also planned this year to increase the internal dimension (vertical) of the undulator vacuum chamber from its present value of 17 mm to the design value of 21 mm. This will facilitate lasing of the IR-FEL at 50 μm wavelength.

A part of the FEL beam is proposed to be coupled to the FTS set-up for the direct measurement of FEL radiation wavelength during the experiments. Subsequently, the experimental station shall be augmented for studies on the temperature, magnetic field and frequency dependence of scattering rate of carriers using IR-Hall measurements. The possibility of pump-probe measurements using FEL light, and the usage of the FEL light for experiments in biology and chemistry are also being explored.

7. Conclusion

The IR-FEL at RRCAT has demonstrated lasing in the 12.5-40.0 μm wavelength range with a maximum CW average out-coupled power of 30 mW, which is five times higher than the design out-coupled power for the present duty-cycle of operation of the machine. This has been possible due to the injector system upgrade, which has successfully delivered up to 0.65 nC charge/micro-pulse in the accelerated electron beam, as compared to the design value of 0.3 nC. First user experiment has been done using the FEL radiation, transported over a distance of 50 m to the user area, by studying the transmission spectra of a silicon standard sample. With an improved transmission of FEL radiation to the user area after the proposed upgrade of the optical beam transport line this year, studies on the temperature, magnetic field and frequency dependence of scattering rate of carriers are proposed to be performed using the facility for IR-Hall measurement. The IR-FEL complements the Indus Synchrotron Radiation Sources at long wavelengths with a brightness $>10^{12}$ photons/s/mm^2/mrad^2/0.1% BW at a nominal operating wavelength of 28 μm, which corresponds to ~40 meV photon energy.

Acknowledgement

The authors acknowledge the contribution of all colleagues of the FUS, on whose behalf this article is being presented. Development of the IR-FEL has been made possible by the very fruitful collaboration with different expert groups at RRCAT, which include the ACSD, AMTD, APSD, BDS, CSD, DMTD, HELOS, LCDFS, LCID, RFSD (including the erstwhile PHPMD), and UHVTS. Colleagues from many other Divisions/Sections have also helped in different aspects of the development activity. The valuable contributions of all these colleagues at RRCAT is very gratefully acknowledged.

References

[1] B. Biswas, U. Kale, M. Khursheed, A. Kumar, V. Kumar, S. Lal, P. Nerpagar, A. Patel and K. K. Pant, "Signature of build-up of coherence in an ingeniously built Compact Ultrafast Terahertz Free Electron Laser set-up", Current Science 105, 1, 26 (2013).

[2] K. K. Pant, "First results from an Infra-red Free Electron Laser (IR-FEL) at RRCAT", RRCAT Newsletter Vol. 29, Issue 2, 2016.

[3] A. Kumar K. K. Pant & S. Krishnagopal, "Simulations and cold-test results of a prototype Plane Wave Transformer linac structure", Physical Review Special Topics - Accelerators and Beams, Vol. 5, 033501, 2002.

[4] K. K. Pant et al., "First lasing in an infrared free electron laser at RRCAT, Indore", Current Science 114, 2, 367 (2018).

[5] A. Kumar et al., "Upgrade of injector system of the IR-FEL at RRCAT", ID-275, Proceedings of Indian Particle Accelerator Conference (InPAC-2018), RRCAT, Indore, Jan. 9-12, 2018.

[6] S. Chandran, A. Kumar, B. Biswas, R. S. Saini, P. Nerpagar and K. K. Pant, "Characterization of the 90 keV Electron Beam and Low Energy Beam Transport in the Upgraded IR-FEL Injector", Proceedings of Indian Particle Accelerator Conference (InPAC-2019), IUAC, Delhi, Nov. 18-21, 2019.

[7] S. Chandran, B. Biswas, S. Lal, A. Kumar, R.S. Saini, M. Khursheed, S.K. Gupta, P. Nerpagar, R.K. Pandit, K.K. Pant, "Commissioning and validation of the injector and electron beam transport systems for the IR-FEL at RRCAT", PRAMANA- Journal of Physics 93, 6, 85 (2019).

[8] S. Chandran, B. Biswas, A. Kumar, R. S. Saini, S. Lal, P. Nerpagar, R. Kumar Pandit, S. Kumar Gupta, U. Kale, K. K. Pant, "The IR-FEL facility at RRCAT: Commissioning experiments and first saturation of lasing at 28 μm wavelength", Nuclear Inst. and Methods in Physics Research, A 1003, 165321 (2021).

[9] W. Fawley, "A user manual for GINGER and its post-processor XPLOTGIN", LBNL- 49625-Rev. I ed., LBNL, 2004.

[10] B. Biswas, S. Chandran, R. S. Saini, T. Dave, S. Lal, A. Kumar, R. K. Pandit, P. Nerpagar, U. Kale, S. K. Gupta and K. K. Pant, "Performance Optimization of the IR-FEL at RRCAT", Proceedings of Indian Particle Accelerator Conference (InPAC-2023), BARC, Mumbai, March 13-16, 2023.

[11] FINESSE Software by A. Freise, University of Birmingham, Source: gwoptics.com.